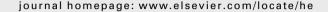
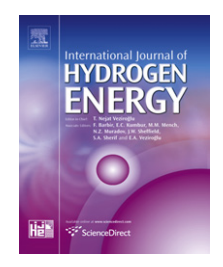


Available at www.sciencedirect.com







Imaging of an operating $LaNi_{4.8}Al_{0.2}$ —based hydrogen storage container

Ł. Gondek ^{a,*}, N.B. Selvaraj ^a, J. Czub ^a, H. Figiel ^a, D. Chapelle ^b, N. Kardjilov ^c, A. Hilger ^c, I. Manke ^c

ARTICLE INFO

Article history:
Received 27 February 2011
Received in revised form
29 April 2011
Accepted 13 May 2011
Available online 14 June 2011

Keywords: Metal-hydride storage systems Neutron radiography Neutron tomography

ABSTRACT

In this paper the phenomena occurring inside of a hydrogen storage container (filled with LaNi $_{4.8}$ Al $_{0.2}$ active material), in operation, are unveiled by means of high-resolution neutron radiography and tomography. Although the metallic hydride-based storage systems are commonly used and commercially available, the processes occurring inside of such devices have been derived rather on the knowledge of several external parameters (changes of $\rm H_2$ pressure or the container's temperature) characterising the whole container than on a direct experimental evidence of the container's interior. The results of neutron imaging experiments reported here show the possibility of qualitative as well as quantitative analysis of hydrogen absorption/desorption kinetics with spatial resolution of 70 μ m. Copyright © 2011, Hydrogen Energy Publications, LLC. Published by Elsevier Ltd. All rights reserved.

1. Introduction

The prospects for application of hydrogen as an energy carrier in the future have caused intensive development of wide range of hydrogen-related applications. Namely, production, efficient storage and recovering of energy from hydrogen are the key problems nowadays [1]. Although the technology of producing and converting gaseous hydrogen into energy is well established, metal-hydride storage systems cannot achieve an efficiency being at the level of at least 10 wt.% (at reasonable thermodynamic conditions) required for common applications. The problems of hydrogen storage are connected mainly with the capacity to weight/volume ratio of hydrogen tanks. Automotive hydrogen storage systems that should have relatively low weight and dimensions may be given as an example.

In fact, there are few methods for hydrogen storage: highpressure gaseous hydrogen vessels, cryogenic liquid-hydrogen

tanks, cryogenic systems relaying on adsorbed hydrogen (MetalOrganic Frameworks – MOF) and metal-hydride based storage systems. Nowadays, high-pressure tanks with carbon fibre coatings, which can withstand pressure up to 700 atm, are constructed [2]. On the other hand, cryogen tanks containing liquid hydrogen at 20 K (–253 $^{\circ}$ C) are also developed. Both of them exhibit quite good hydrogen storage properties, nevertheless the factors such as safety or technological advancement can be considered as drawbacks. Recent developments in MOF storage systems, where an adsorption of molecular hydrogen onto mesoporous structures (up to 10 wt.%) takes place at temperatures of liquid nitrogen (77 K, -196 °C), give a chance of replacing liquid hydrogen storage systems [3,4]. For economical and safety reasons great attention is paid to the materials exhibiting high hydrogen absorption like metal-hydrides or chemical compounds which may release hydrogen quite easily [5]. Such materials can store hydrogen at pressures not much

^a AGH University of Science and Technology, Faculty of Physics and Applied Computer Science, al. A. Mickiewicza 30, 30-059 Krakow, Poland

^b Insitut FEMTO ST, Dépt. de Mécanique Appliquée Raymond Chaléat, Université de Franche-Comte, 25000 Besancon, France

^cHelmholtz Center Berlin for Materials and Energy, Hahn-Meitner Platz 1, D-14109 Berlin, Germany

^{*} Corresponding author.

higher than atmospheric (up to few bars) with comparable or higher volume capacity than in the case of pressure and cryogen tanks (50-60 gH₂/l for typical pressure tanks, 70 gH₂/l for liquid storage, 115 gH₂/l for LaNi₅). Apart from typical methods of hydrogen storage, a concept of hybrid storage systems has been issued. In principle, it combines high-pressure vessels capability with the capability of some alloy-based hydrogen storage materials that absorbs hydrogen under elevated pressures [6]. Apparently, the performance of traditional metalhydride or hybrid storage systems is strongly affected by the internal structure of the tank which is also responsible for heat transport along the container and accessibility of the active material to the hydrogen. These parameters influence directly the hydrogen absorption/desorption kinetics, therefore they are crucial for a convenient (fast) operation at the highest possible efficiency. The comprehensive review of the hydrogen energy problems mentioned above may be found in Ref. [1].

In contrast to X-rays, neutrons possess properties that make them perfectly suited for the investigation of processes inside hydrogen storage tanks [7]. In principle, the attenuation of the beam passing through an object is described by the Lamber-Beer law:

$$I = I_0 e^{-\sum d} \tag{1}$$

where I_0 is an incident beam intensity, Σ is the linear attenuation coefficient and d is the width of the sample. The Σ coefficient depends on the appropriate scattering and absorption cross sections and on the density of the scattering centres. The Σ coefficient for neutrons is not connected with the atomic number as in the case of X-rays. It depends on the nucleus structure of the particular atom. Therefore, the hydrogen nuclei exhibit one of the highest attenuation among the elements. This provides excellent contrast of two orders of magnitude between hydrogen and common metals as Al, Ni, Cu, etc. These specific features make containers made of aluminium transparent for the neutron beam (even for the wall thickness exceeding 10 mm). In addition, the LaNi5-based alloys are quite transparent to the neutron beam as well. In case of X-rays, hydrogen is practically invisible while even a thin metallic absorber stops the beam completely.

Surprisingly enough, there are only a few publications that raise the issue of the hydrogen absorption by metallic systems studied by neutron imaging techniques. The results reported there were obtained for the ex-situ hydrogenated materials that were used for specimen preparation [8-11]. The gained knowledge, extremely important for the basic research on hydrides, did not contribute significantly to the issue of storage systems. However, it must be underlined that those papers established usefulness of neutron imaging techniques for the further studies of hydrogen-absorbing alloys. To the best of our knowledge, there are just two journal-publications concerning in-situ measurements [12,13]. In the second publication for the first time the problem of neutron imaging of hydrogen storage is treated quantitatively. The resolution of the experiment reported there was limited to 0.25 mm in order to keep sufficient beam intensity for fast kinetics studies. We strongly believe that those contributions (including the current one) will be an encouragement to the wider use of neutron imaging techniques in this field.

2. Experimental

2.1. Neutron imaging techniques

Neutron imaging experiments were performed at the research reactor of the Helmholtz Centre Berlin for Materials and Energy (HZB) using the cold neutron high-resolution CONRAD (V7) instrument [14]. Cold neutrons offer better contrast due to enhancement of the absorption ratio than thermal ones. The incident cold-neutrons beam has a broad Maxwellian-like spectrum with wavelengths between about 0.2 and 1.2 nm with a maximum at 0.35 nm. A 10 mm pinhole was used and the flight path between sample and a pinhole was 5 m. Therefore, the L/D collimation ratio was about 500, what reduces image blurring and ensures high spatial resolution. The resolution tests performed prior to the main experiment yielded a spatial resolution of 70 µm. The beam dimensions allow investigations of objects with dimensions up to approximately 100 mm × 100 mm. The sample was mounted on a goniometric table enabling rotation and translation along two axes. Just behind the sample a scintillating screen is placed, where neutrons are converted into the visible light. The light beam is then reflected by a mirror to prevent radiation damage on the CCD camera and its electronics. After passing through the focusing optical system, photons are detected by a CCD camera (Andor DW436N-BV) with the resolution of 2048 \times 2048 pixels. The CCD camera was cooled by Peltier elements (-70 °C) in order to keep spurious signals at the lowest level. The exposure times used for the experiments were 10 or 30 s for every projection image in the radiography experiments and up to 45 s in the tomography experiments. The sketch of the experimental stage is given in Fig. 1.

Before starting each experiment, a dark field image (DFI) and a flat field image (FFI) were recorded. A DFI image was recorded with the neutron beam stopped in order to check the dark currents in the CCD camera. An FFI image was collected in order to record a distribution of the beam without the sample. The difference between FFI-DFI images can be attributed directly to the incident beam intensity (Io according to the eq. (1)). On the other hand, the image of the investigated object after subtracting the DFI image can be interpreted as the transmitted beam intensity (I according to the eq. (1)). By simple dividing of I/ I₀ the attenuation coefficient can be calculated. Consequently, with the knowledge of the appropriate cross sections for neutron absorption and scattering, the density of the absorbent may be calculated. However, it must be noted that the obtained information is integrated along the path of the neutron within the sample.

Neutron tomography studies require collecting of a few hundred of radiographic projection images of the investigated object at different orientations with respect to the incident beam. In our case 400 images were recorded covering the 0–180° rotation range for each reconstruction. The rotation axis was perpendicular to the beam and in the geometrical centre of the investigated object. The reconstruction, which was based on those images, was made using the filtered back-projection algorithm. The final reconstruction consists of a fully 3D distribution of the attenuation coefficient. Therefore, the quantitative calculations are possible similarly to the radiographic case. However, using tomographic reconstructions one gets the

Download English Version:

https://daneshyari.com/en/article/1278916

Download Persian Version:

https://daneshyari.com/article/1278916

<u>Daneshyari.com</u>